IIT Madras

Final year BTech Project

Lattice Boltzmann simulation of evaporating droplet

Aqel Ahammad K P
CH13B006

Guided by
Prof. Sumesh Thampi

March 2, 2017

Contents

1 Governing equations

Continuity equation,

$$\frac{\partial \rho}{\partial t} + \nabla.(\rho \vec{v}) = 0 \tag{1}$$

Navier-Stokes equation,

$$\rho[\vec{v} + (\vec{v}.\nabla)\vec{v}] = \eta \nabla^2 \vec{v} - \phi \nabla \mu - \nabla P \tag{2}$$

Cahn-Hilliard convection-diffusion equation,

$$\frac{\partial \phi}{\partial t} = \nabla.(\phi \vec{v}) + \nabla.(M \nabla \phi) \tag{3}$$

where ϕ is the phase field and M is *mobility parameter* which plays the role of diffusivity.

2 Lattice-Boltzmann method

Instead of solving equations (1)-(3), the discrete Boltzmann equation is solved to simulate the flow of a Newtonian fluid.

$$f_i(\mathbf{r} + \mathbf{c}_i \Delta t, t + \Delta t) - f_i(\mathbf{r}, t) = -\frac{\Delta t}{\tau}(f_i - f_i^{eq}) \tag{4}$$

$$g_i(\mathbf{r} + \mathbf{c}_i \Delta t, t + \Delta t) - g_i(\mathbf{r}, t) = -\frac{\Delta t}{\tau_g}(g_i - g_i^{eq}) \tag{5}$$

Hydrodynamic variables are related to above velocity distribution functions by,

$$\rho \equiv \sum_i f_i, \quad \rho v_\alpha \equiv \sum_i c_{i\alpha} f_i, \quad \phi \equiv \sum_i g_i \tag{6}$$

Also,

$$\sum_i f_i^{eq} \equiv \rho, \quad \sum_i c_{i\alpha} f_i^{eq} \equiv rho v_\alpha, \sum_i g_i^{eq} \equiv \quad \phi \tag{7}$$

Expressions for equilibrium distribution functions are reported in [1].

3 Spinodal decomposition

Spinodal decomposition is a mechanism for the rapid unmixing of a mixture of liquids or solids from one thermodynamic phase, to form two coexisting phases. Refer Figure 1 for the spinodal decomposition simulation where we started with each point having a random ϕ value where $-1 \leq \phi \leq 1$.

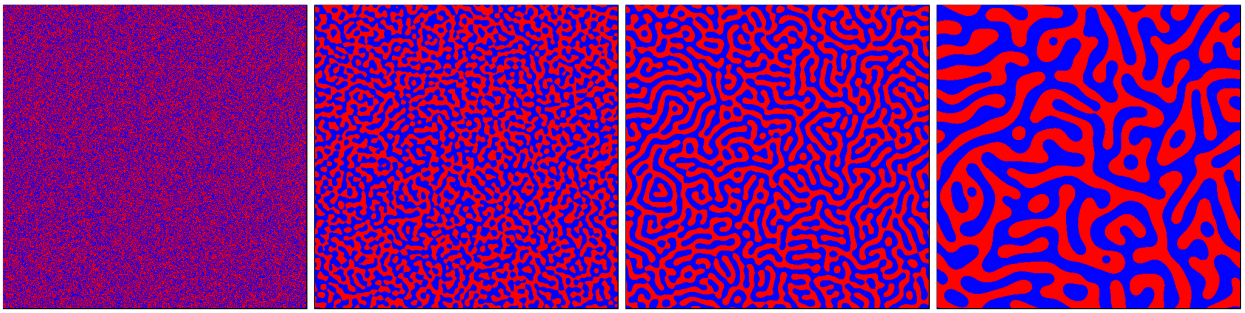

(a) t = 0 (b) t = 1000 (c) t = 10000 (d) t = 100000

Figure 1: Spinodal decomposition simulation in a domain of 500 * 500 using Lattice Boltmann method. It can be seen that phases unmix to form sepearte clusters.

[Click here to see the video of the simulation.]

4 Surface tension

Surface tension is the elastic tendency of a fluid surface which makes it acquire the least surface area possible. For any volume, sphere gives the least surface area. In the following simulation, a cubic volume of liquid is taken at t = 0. As expected, the droplets changes itself to a spherical droplet. (Refer Figure 2)

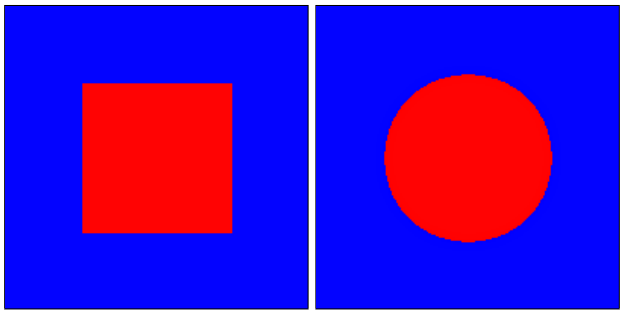

(a) At t = 0 (b) At equilibrium

Figure 2: Evolution of a square surface to a circular surface.

5 Variation of phase phield close to interphase

Close to interface, the phase field varies as a hyperbolic tangent with the normal cordinates to the interface, r. Simulation data was perfectly matching with the numberical solution given by [2]. (Refer Fig 3)

$$\phi(r) = \phi_{eq} tanh(\frac{r}{\epsilon}) \tag{8}$$

where $\phi_{eq} = \sqrt{-a/b}$ and $\epsilon \equiv \sqrt{-2k/a}$ is the interface thickness

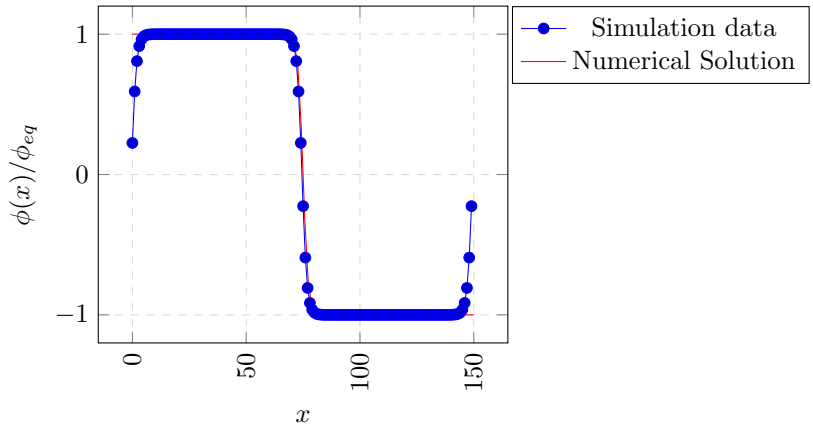

Figure 3: Phase field profile along normal to interface of two already seperated phases

6 LB Method and Method of Lines

Equation (3) can be solved using method of lines, and the above simulations can be achieved. In this section, we compare various aspects of algorithms of LB method(LBM) and method of lines(MOL)

Time complexity

Average time required for one iteration in both the algorithms was noted and plotted in Figure 4a. It was noted that time for one iteration of MOL is almost equal to LB method with D2Q9 lattice. Time varies linearly with number of points for both the algorithms. Hence both shows time complexity of $\mathcal{O}(n)$

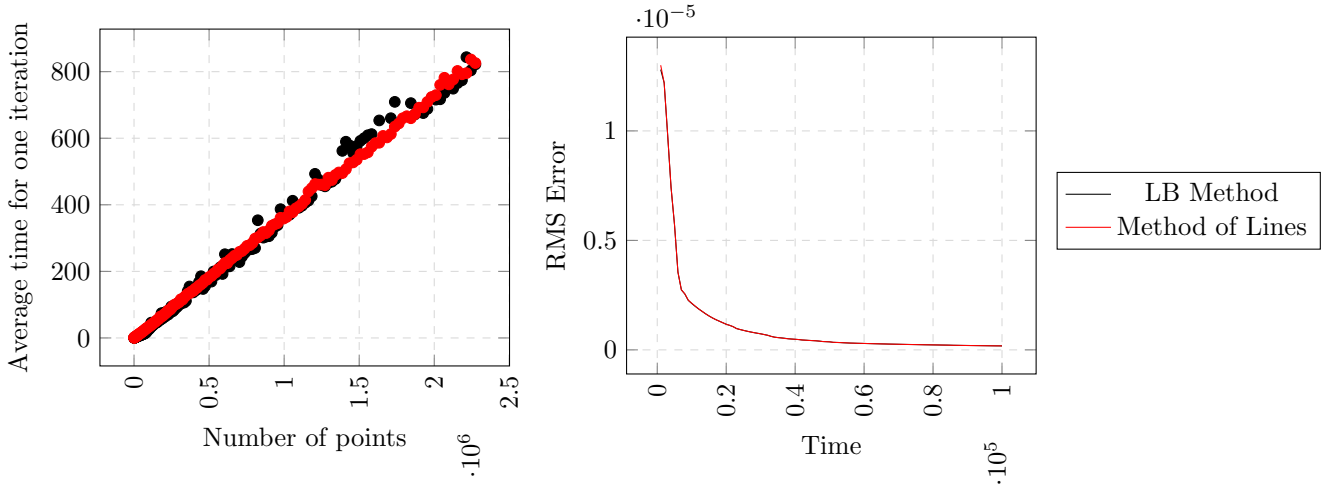

(a) Average time for one iteration vary linearly for both the methods

(b) Both the algorithms show same time for convergence

Figure 4: Time complexity and convergence analysis for LB method and method of lines

Space complexity

Both the algorithms have same space complexity $\mathcal{O}(n)$

Time for convergence

It was noted that both the methods gives almost same result and error at a particular time and takes almost same time to converge to a solution.

7 Solid wall

Bounce-back rules [3] are imposed along the boundary for impenetrability and no-slip boundary conditions. Also,

$$\vec{n}.\nabla\mu = 0 \tag{9}$$

For an equilibrium contact angle on an ideal solid wall, geometrical formulation is used for implemeting wetting condition [4].

$$\phi_{i,j,1} = \phi_{i,j,3} + tanh(\frac{\pi}{2} - \theta)\xi \tag{10}$$

where

$$\xi = \sqrt{(\phi_{i+1,j,2} - \phi_{i-1,j,2})^2 + (\phi_{i,j+1,2} - \phi_{i,j-1,2})^2} \tag{11}$$

Considering the shape of the droplet, contact angle is given by[5]

$$tan(\theta) = \frac{b_0}{2(R - a_0)} \tag{12}$$

where a_0 is the droplet height and b_0 is the wet length between the droplet and the wall,

$$R = \frac{a_0}{2} + \frac{b_0^2}{8a_0} \tag{13}$$

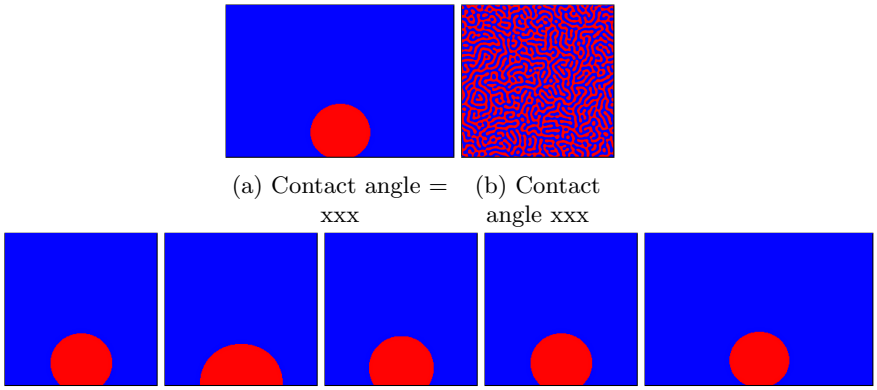

(a) Contact angle = xxx (b) Contact angle xxx

(c) Contact angle = xx^0 (d) Contact angle = 90^0 (e) Contact angle = 120^0 (f) Conatact angle = 135^0 (g) Contact angle = 150^0

Figure 5: Droplets on solid wall with different contact angles

8 Evaporation of a planar droplet

To drive evaporation of the film we impose the boundary condition $\phi(z = z_H, t) = \phi_H$, where $\phi_H < -\phi_{eq}$. This induces a gradient in the chemical potential field μ. In response to this imabalance, the system reduces ϕ, which curresponds to the evaporation of the film[6]. Phase field imbalance, $\Delta\phi_H \equiv -\phi_{eq} - \phi_H$
We performed simulations in a box consisting of 1 x 1 x 150 lattice sites. Periodic boundary conditions were set in the x and y directions. A wall was located at $z_w = 1$, while the concentration was fixed to a value ϕ_H at $z_H = N_z$ to drive the system out of equilibrium. The initial height of the film was set to $z_0 = 100$.

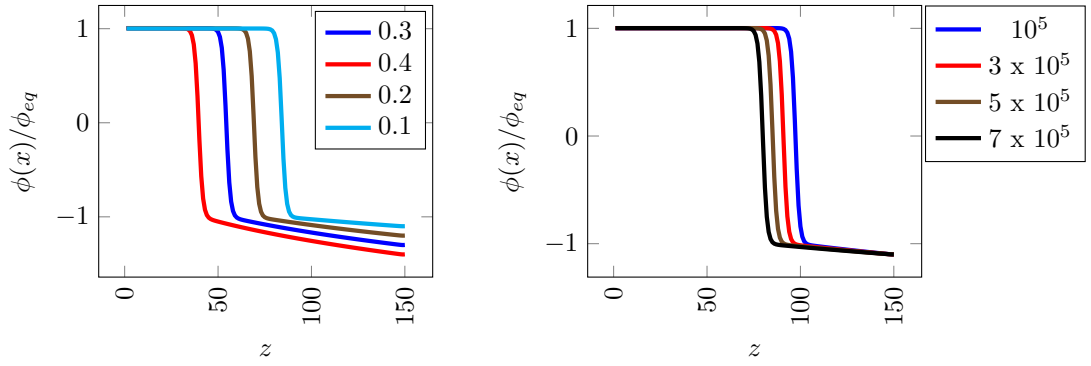

(a) After 5 x 10^6 simulation steps with different ϕ_H (b) Phase field profile at different time steps

Figure 6: Phase field profile for the planar film evaporation.

9 Evaporation of a droplet on solid wall

Refer Figure 7

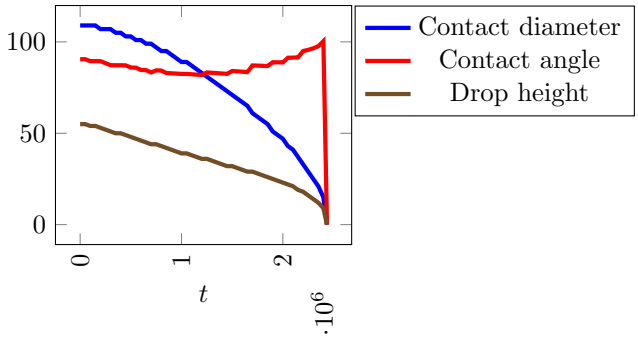

Figure 7: Evaporation of a droplet with contact angle 90^0 for $\nabla\phi_H = 0.1$.

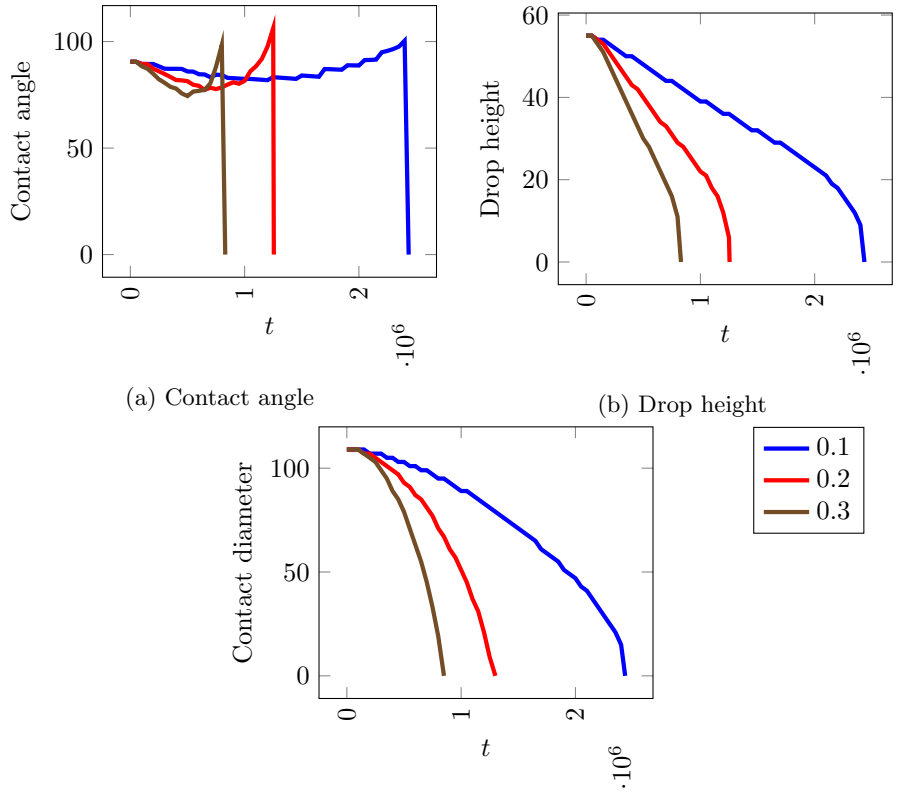

(a) Contact angle

(b) Drop height

(c) Contact diameter

Figure 8: Evaporation of a droplet on a surface with contact angle 90^0 for different $\nabla\phi$.

References

[1] J.-C. D. I. P. P. B. V. M. Kendon, M. E. Cates, "Inertial effects in three dimensional spinodal decomposition of a symmetric binary fluid mixture: A lattice boltzmann study," *J. Fluid Mech. 440 (2001) 147-203*, 2000.

[2] I. P. P.T. Sumesh and R. Adhikari, "Lattice boltzmann - langevin simulations of binary mixtures," *Phys. Rev. E 84, 046709 (2011)*, 2011.

[3] A. J. C. L. Verberg, "Lattice-boltzmann simulations of particle-fluid suspensions," *Journal of Statistical Physics*, vol. 104, no. 5, pp. 1191–1251, 2001.

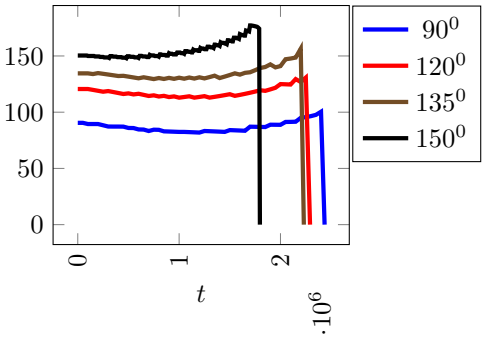

Figure 9: Evaporation of a droplet with different contact angles for $\nabla\phi_H = 0.1$.

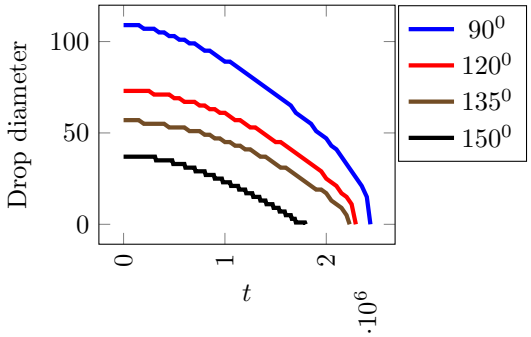

Figure 10: Evaporation of a droplet with different contact angles for $\nabla\phi_H = 0.1$.

[4] H.-b. H. Lei Wang and X.-Y. Lu, "Scheme for contact angle and its hysteresis in a multiphase lattice boltzmann method," *Phys. Rev. E 87, 013301*, 2013.

[5] Q. Kang, D. Zhang, and S. Chen, "Displacement of a two-dimensional immiscible droplet in a channel," *Physics of Fluids*, vol. 14, no. 9, pp. 3203–3214, 2002.

[6] R. Ledesma-Aguilar, D. Vella, and J. M. Yeomans, "Lattice-boltzmann simulations of droplet evaporation.," *Soft Matter*, vol. 10, no. 41, pp. 8267–8275, 2014.